

STUDY ON SELECTIVE LASER MELTING OF COPPER

Luiza Bertoldo Benedetti, luizabenedetti@gmail.com¹
Cleiton André Comelli, cleiton.comelli@gmail.com¹
Carlos Henrique Ahrens, carlos.ahrens@ufsc.br¹

¹ Universidade Federal de Santa Catarina (UFSC), R. Eng. Agrônomo Andrei Cristian Ferreira, s/n - Trindade, Florianópolis - SC, 88040-900.

Abstract. *Selective laser melting (SLM) is one of the most popular additive manufacturing (AM) technologies for the manufacture of metal parts from a CAD representation. One investigation of interest in this field is the fabrication of copper components. In this study cube specimens were manufactured with varied parameters, in terms of layer thickness, scanning speed and remelting. The investigation aimed to obtain the highest consolidation for copper, a difficult material to process due to its high thermal conductivity and lower laser absorption coefficient. The best parameters of processing were obtained by using an energy application between approximately 50 and 300 J/mm³. The results showed that a higher energy application produced warpage, and a lower application of energy resulted in non-densified specimens. The specimens were characterized by evaluating their hardness and microstructure. The results were analyzed under ANOVA method, which showed a weak correlation between consolidation and hardness, while the analysis of the microstructure supported the low mechanical properties obtained with the samples if compared to solid pure copper.*

Keywords: Additive Manufacturing, Selective Laser Melting, Copper.

1. INTRODUCTION

Additive Manufacturing (AM) has significantly emerged in the last three decades as an alternative process of manufacturing in which material is joined together to create objects from a 3D model data, usually layer upon layer (ASTM International 2015; Kruth et al. 2007; Thompson et al. 2015). Among these techniques, Selective Laser Melting (SLM) has shown a high potential in rapid manufacturing due to its capability of generating serial products with reproducible properties (Drummer et al. 2012). SLM technique uses one or more lasers to manufacture 3D parts by fusing or sintering powder on a fixtureless table, layer by layer, according to their CAD representation (ASTM International 2015; Bourell et al. 2014). It offers other advantages, such as flexibility, cost reduction, extended part/tool life and it may increase surface resistance to wear and fatigue as well as reduce environmental impacts. Furthermore, in comparison to other AM systems, SLM can manufacture complex and unique parts in a quite wide range of materials, including metals, even though limitations are still visible (Bourell et al. 2014).

According to previous literature, copper samples were hard to manufacture by SLM and did not obtain full density (D. Gu et al. 2007; Lykov P.A., Safonov E.V. 2016; Popovich et al. 2016; Tang et al. 2003; Zhu, Lu, and Fuh 2003). The authors claim that both copper high thermal coefficient and high reflectivity are the main reasons which prevent achieving high consolidation, therefore better mechanical performance (Lykov P.A., Safonov E.V. 2016; Popovich et al. 2016; Tang et al. 2003; Zhu, Lu, and Fuh 2003). However, Lykov P.A. et al (2016) and Vinod A.R. (2014) concluded that by applying lower scan speed and higher laser power, which result in higher energy application, may improve relative density of copper samples (Lykov P.A., Safonov E.V. 2016; Vinod and Srinivasa 2014). If a good density of copper is achieved by SLM, this material can be used to produce heat pipes, mold inserts, electrodes and aviation and military devices (Liu et al. 2014; Popovich et al. 2016; Vinod and Srinivasa 2014).

Lykov P.A. et al. (2016) and Vinod A.R. (2014) performed the experiments with the assistance of a CO₂ laser, known to have a wavelength range close to 10.6 μm (Santos et al. 2006), thus ten times larger than the wavelength best absorbed by metals. To better understand the behaviour of this material the present work used fiber laser to manufacture pure copper powder by SLM. It aimed to achieve a maximum density, taking into account the machine power limit output of 94 W in order to obtain a high mechanical performance. The specimens' characterization included consolidation, Scanning Electron Microscopy (SEM) analysis and the evaluation of microstructure and hardness.

2. EXPERIMENTAL METHOD

2.1. Copper powder characterization

Copper powder from *Combustol Metalpó* was selected for this study. This powder is typically used to manufacture sintered heat pipes, and is obtained by moulding of uniaxial compression. EDX analysis was performed in a JEOL JSM-6390LV machine with 15.0 kV of accelerating voltage. As depicted in Figure 1, the powder analyzed showed a composition of approximately 93% of copper with some impurities identified in the energy-dispersive x-ray spectroscopy (EDX) as carbon (5%), oxygen (1%) and aluminum (1%)

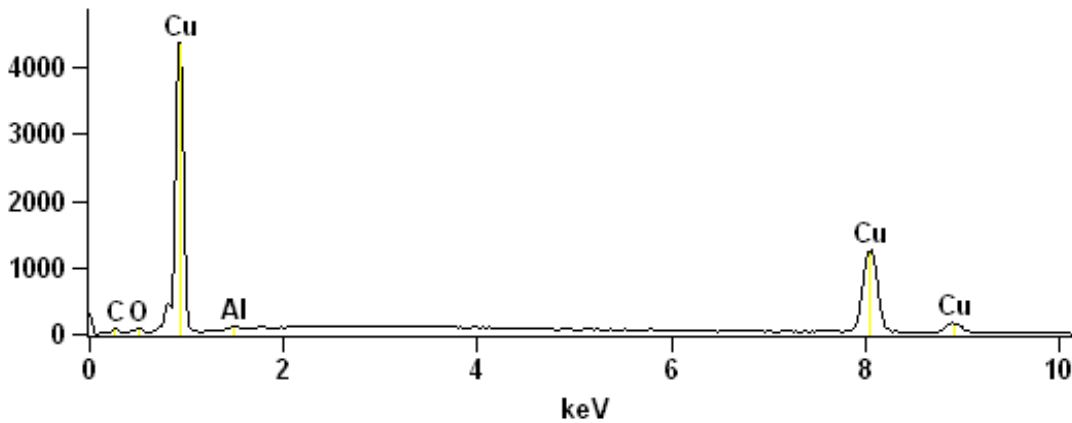
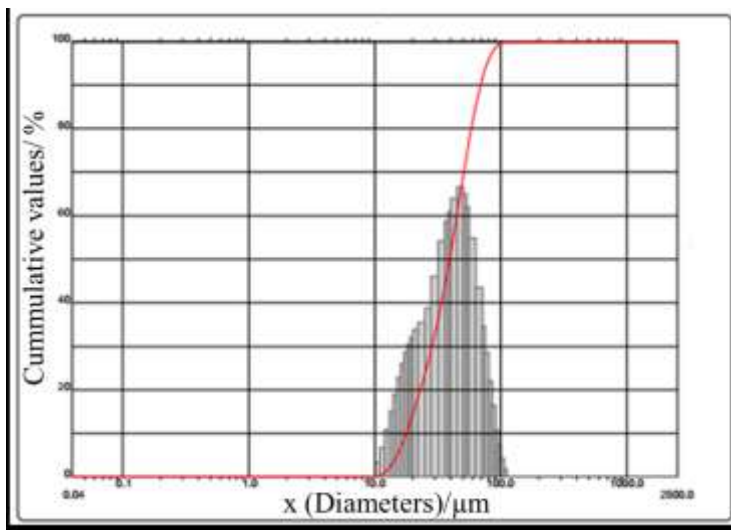


Figure 1: EDX of the copper powder studied.

A Cilas 1190 machine was used to evaluate the particle size distribution. The powder has an average particle size distribution of 41.66 μm and presented the histogram of the particles distribution showed in Figure 2.



| | |
|------------------|---------------------|
| Diameter in 10% | 17.72 μm |
| Diameter in 50% | 39.23 μm |
| Diameter in 90% | 69.23 μm |
| Average diameter | 41.66 μm |

Figure 2: Particle size distribution of the copper powder used in the study.

The particles were also taken to SEM analysis. Figure 3 shows a quite heterogeneous structure of particles, typical from water atomization process. The particles are not round and even though the particle size distribution analysis shows a Gaussian distribution, it is visible that a few particles can achieve a size up to 200 μm while the majority presents a diameter close to 50 μm . This morphology suggests that it can compromise the process, preventing good flowability of the powder over the building area. The energy required may be necessary to increase due to the size of some particles, which might need more energy to sinter and consolidate into a solid structure.

The powder was taken to flowability test, which was performed with the assistance of a Hall funnel according to ASTM B213-13 (ASTM International 2013). The powder did not flow as desired, remaining on the funnel. In order to enable the process, a helical system was coupled in the machine to push the powder forward until it falls on the dragging system (see Figure 4).

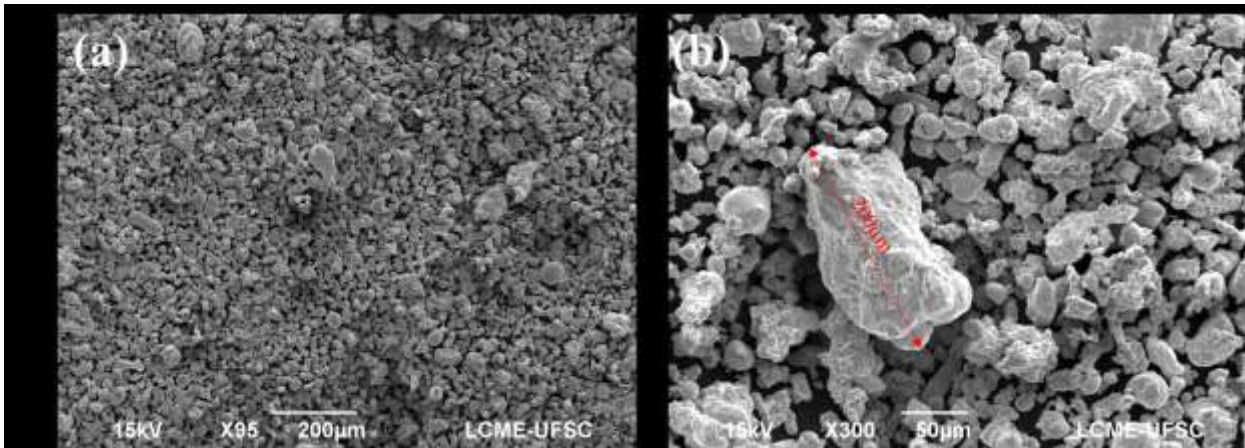


Figure 3: SEM analysis of copper powder; (a) 95x (b) 300x of magnification

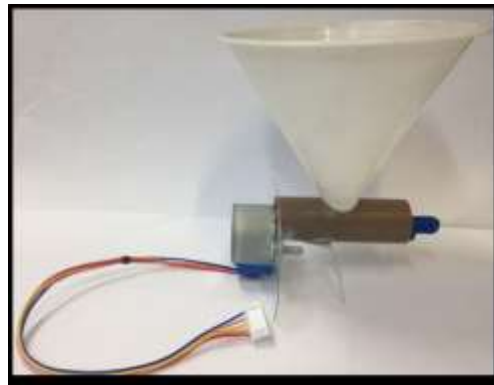


Figure 4: Helicoïdal system used to spread the powder in the study.

2.2. SLM Machine

The SLM machine used was a non commercial machine, containing a powder deliver and distribution system, a building chamber containing a stainless steel platform (substrate) and a fiber laser of 94 W of power output, 1.06 µm and capable of scanning speeds up to 7000 mm/s. All the atmosphere during the building process is controlled with argon, so that no more than 0.5% of oxygen is found during operation. To facilitate the use of copper powders, the deliver system is equipped with a funnel containing a helicoïdal system, as already shown in Figure 4.

2.3. Specimens dimensions and parameters of fabrication

Cube specimens with dimensions 10x10x5mm were manufactured. The parameters were selected according to literature, taking into account density of energy and scanning speed. The minimum scanning speed found in literature for copper alloy manufactured by SLM was used by Lykov P.A et al (2016) and Gustmann T. et al (2016), and is 100 mm/s (Gustmann et al. 2016; Lykov P.A., Safonov E.V. 2016). However, Lodes M. A. (2015) applied scanning speeds up to twenty times higher (Lodes, Guschlbauer, and Korner 2015). The density of energy was also variable: from 40 J/mm³ (Zhu, Lu, and Fuh 2003) to 300 J/mm³ (Lodes, Guschlbauer, and Korner 2015). These works used a power output range from 50 W (Gustmann et al. 2016) to 400 W (Popovich et al. 2016). The lack of power was balanced by applying lower scanning speeds according to Eq. (1), which has been used many times in literature (Berzins, Childs, and Ryder 1996; Childs et al. 1999; Childs and Tontowi 2001; Franco, Lanzetta, and Romoli 2010; D. D. Gu et al. 2012; Hon and Gill 2003; Schmidt, Pohle, and Rechtenwald 2007) and suggests the relation between the machine parameters and energy application as,

$$VED = P/vhs \tag{1}$$

in which:

VED = Volumetric Energy Density (J/mm^3);

P = Laser power (J);

v = Scanning speed (mm/s);

h = hatch distance (mm);

s = layer thickness (mm).

The analysis of variance method was used to select the initial parameters and determine the minimum and maximum energy required for copper specimens' production. Firstly, 30 different combinations of parameters were selected by varying scanning speed, from 20 to 200 mm/s, layer thickness (0.075 mm or 0.1 mm) and the remelting technique (no remelting, remelting once, remelting twice). The parameters limits chosen took into account literature review, especially the material, upper and lower limit of scanning speed and total volumetric energy density. The remelting technique was applied because few studies have explored the reapplication of energy on the same layer (Gustmann et al. 2016; Popovich et al. 2016; da Silva et al. 2016) and the results have proved to be an alternative solution for good consolidation and mechanical results achievement (da Silva et al. 2016), especially if power output is constrained. In this study, the remelting once or twice was evaluated, respectively, as twice and three times the volumetric energy applied according to Eq. (1), even though it might not be equivalent. For all specimens the power selected was 94 W and the hatch distance was 0.1 mm, since similar values were used frequently in literature to manufacture copper powder by SLM process (Gustmann et al. 2016; Lodes, Guschlbauer, and Korner 2015; Lykov P.A., Safonov E.V. 2016; Popovich et al. 2016).

Some combination of parameters did not produce specimens due to the high amount of energy applied, causing warpage as a result of high cooling rate. Energies above $290 J/mm^3$ and below $47 J/mm^3$ did not produce completed specimens; similar results were found in literature (Gustmann et al. 2016; Liu et al. 2014; Lodes, Guschlbauer, and Korner 2015; Lykov P.A., Safonov E.V. 2016; Popovich et al. 2016; Vinod and Srinivasa 2014). The volumetric energy density excluded 12 combination of parameters from the DOE, remaining 18 combinations to be evaluated by means of consolidation, microstructure and hardness. The combinations are given in Table 1.

Table 1: Combination of parameters used in each specimen of the DOE.

| Sample | Scanning Speed (mm/s) | Layer thickness (mm) | Remelting ⁽¹⁾ | Volumetric Energy Density (J/mm^3) |
|--------|-----------------------|----------------------|--------------------------|--|
| 1 | 155 | 0.075 | 0 | 80.86 |
| 2 | 65 | 0.1 | 1 | 289.23 |
| 3 | 200 | 0.1 | 2 | 141 |
| 4 | 110 | 0.075 | 0 | 113.94 |
| 5 | 110 | 0.1 | 2 | 256.36 |
| 6 | 200 | 0.075 | 1 | 125.34 |
| 7 | 200 | 0.1 | 1 | 94 |
| 8 | 110 | 0.1 | 0 | 85.45 |
| 9 | 200 | 0.075 | 2 | 188 |
| 10 | 155 | 0.075 | 1 | 161.72 |
| 11 | 155 | 0.1 | 2 | 181.94 |
| 12 | 65 | 0.075 | 0 | 192.82 |
| 13 | 110 | 0.1 | 1 | 170.91 |
| 14 | 155 | 0.1 | 0 | 60.65 |
| 15 | 155 | 0.1 | 1 | 121.30 |
| 16 | 65 | 0.1 | 0 | 144.62 |
| 17 | 200 | 0.075 | 0 | 62.67 |
| 18 | 200 | 0.1 | 0 | 47 |

⁽¹⁾ Remelting number refers to the number the scan passes in addition to the usual scanning count.

2.4. Consolidation

Initially the method used to measure consolidation was Archimedes. However, due to high porosity found in many of the specimens, water was permeating the interstitial porous even when grease was used to cover the surface. It was then decided to apply the volumetric method to measure consolidation. A Mitutoyo digital caliper and a Sagar digital lab scale were used. All the specimens were measured in the same day in order to reduce systematic errors.

2.5. Microstructure

Six specimens were taken to SEM analysis. The equipment used was a JEOL JSM-6390LV microscope. The same specimens were also taken to optic microscopy and were etched according to ASTM No. 30, an ammonia solution, in order to evaluate the grain size and general microstructure. A Leica DM4000 M LED optical microscope was used to analyze the microstructure.

2.6. Hardness

To measure hardness, an Emco-Test hardness testing equipment was used with pre-load of 31.25 N and principal load of 306.56 N. Brinell method was chosen due to the heterogeneities of the samples, which could give a very different result in different locations. Brinell method applies the force in a bigger area, collecting a more realistic result.

3. RESULTS AND DISCUSSION

Figure 5 shows some copper specimens under manufacture and adhered to the substrate.

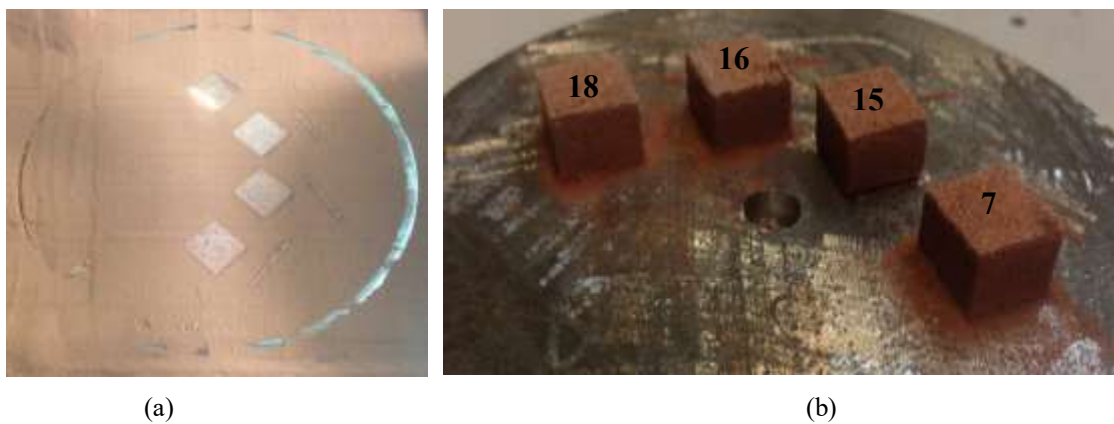


Figure 5: Specimens of copper; (a) Under manufacture, (b) adhered to the substrate (stainless steel).

The specimens adhered slightly to the substrate, possibly as a result of low interaction between copper and stainless steel, the material of the substrate. Z.H. Liu et al. (2014) showed a narrow diffusion zone for copper alloy and stainless steel, even at high temperatures (Liu et al. 2014). By applying some energy in order to heat the substrate before applying the first layer of copper powder it was possible to achieve a better adhesion, therefore completing the specimens manufacture without dragging them out of the platform. Table 2 shows the volumetric consolidation obtained for the specimens manufactured in this study.

Table 2: Consolidation of copper specimens

| Sample | Volumetric Energy Density (J/mm ³) | Consolidation (%) |
|--------|--|-------------------|
| 1 | 80.86 | 47.72 |
| 2 | 289.23 | 47.33 |
| 3 | 141 | 46.58 |
| 4 | 113.94 | 48.91 |
| 5 | 256.36 | 45.19 |
| 6 | 125.34 | 45.95 |
| 7 | 94 | 43.41 |
| 8 | 85.45 | 44.03 |
| 9 | 188 | 45.71 |
| 10 | 161.72 | 48.01 |
| 11 | 181.94 | 43.35 |
| 12 | 192.82 | 48.57 |
| 13 | 170.91 | 47.09 |

| | | |
|----|--------|-------|
| 14 | 60.65 | 43.24 |
| 15 | 121.3 | 44.87 |
| 16 | 144.62 | 47.27 |
| 17 | 62.67 | 46.65 |
| 18 | 47 | 42.66 |

Specimen 4 has presented the best consolidation with approximately 51% of porosity. The energy applied in this specimen was intermediate and a bit lower when compared to the energy applied in literature for copper material (Lodes, Guschlbauer, and Korner 2015; Lykov P.A., Safonov E.V. 2016; Popovich et al. 2016). Similar densification was achieved with other energies, such as for specimens 10 and 12, concluding that parameters with an energy application between 100 and 200 J/mm³ resulted in better consolidation.

Some parameters, however, seem to influence more on the densification than others. The DOE analysis shows that a remelting might contribute to particle densification, however, a double remelting may interfere in the material capability to densify. The other two parameters performed an expected result when considering Eq. (1) - lower scanning speeds tend to increase density, while a layer thickness of 0.075mm showed better results than a layer thickness of 0.1mm. The DOE plot for main effects on densification is shown in Figure 6.

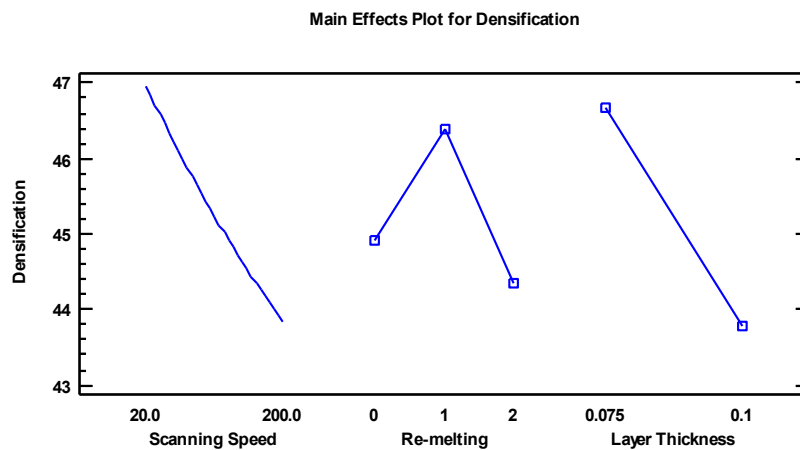


Figure 6: Main effects plot for densification of copper.

Evaluating the influence of each parameter and the combination of parameters through Pareto Chart (Figure 7), it is possible to conclude that the combination has a more relevant effect than the parameters themselves. Scanning speed and remelting have shown a major importance on densification, followed by the combinations of layer thickness and remelting. Remelting is the main single parameter on densification, followed by scanning speed, and lastly, layer thickness.

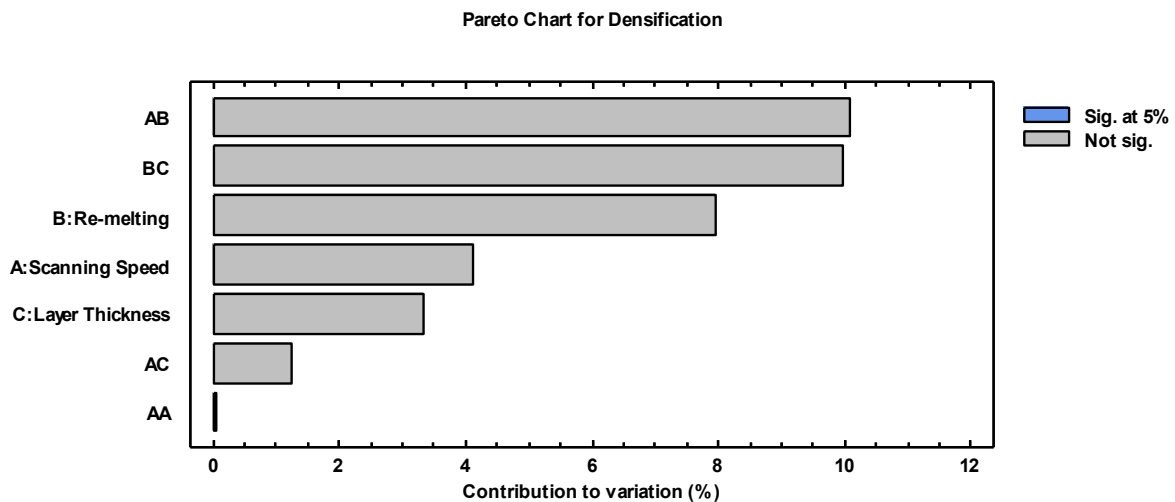


Figure 7: Pareto Chart for copper specimens.

In previous literature the main parameters of influence were usually power output (Gustmann et al. 2016; Tang et al. 2003) and scanning speed (Gustmann et al. 2016; Vinod and Srinivasa 2014). This study has shown that remelting also has an important role on consolidation and must be explored more deeply.

The specimens were taken to SEM analysis in order to evaluate general layer consolidation and direction of welding. The samples selected were 2-4, 6, 12 and 18 (Figure 8). Samples 2 and 18 were chosen in order to compare maximum and minimum energy applied, respectively; samples 6 and 12 were analyzed in order to compare minimum and maximum scanning speed applied; sample 3 was chosen with the aim to compare the remelting application with sample 18; and sample 4 was picked because it obtained the highest consolidation among the samples.

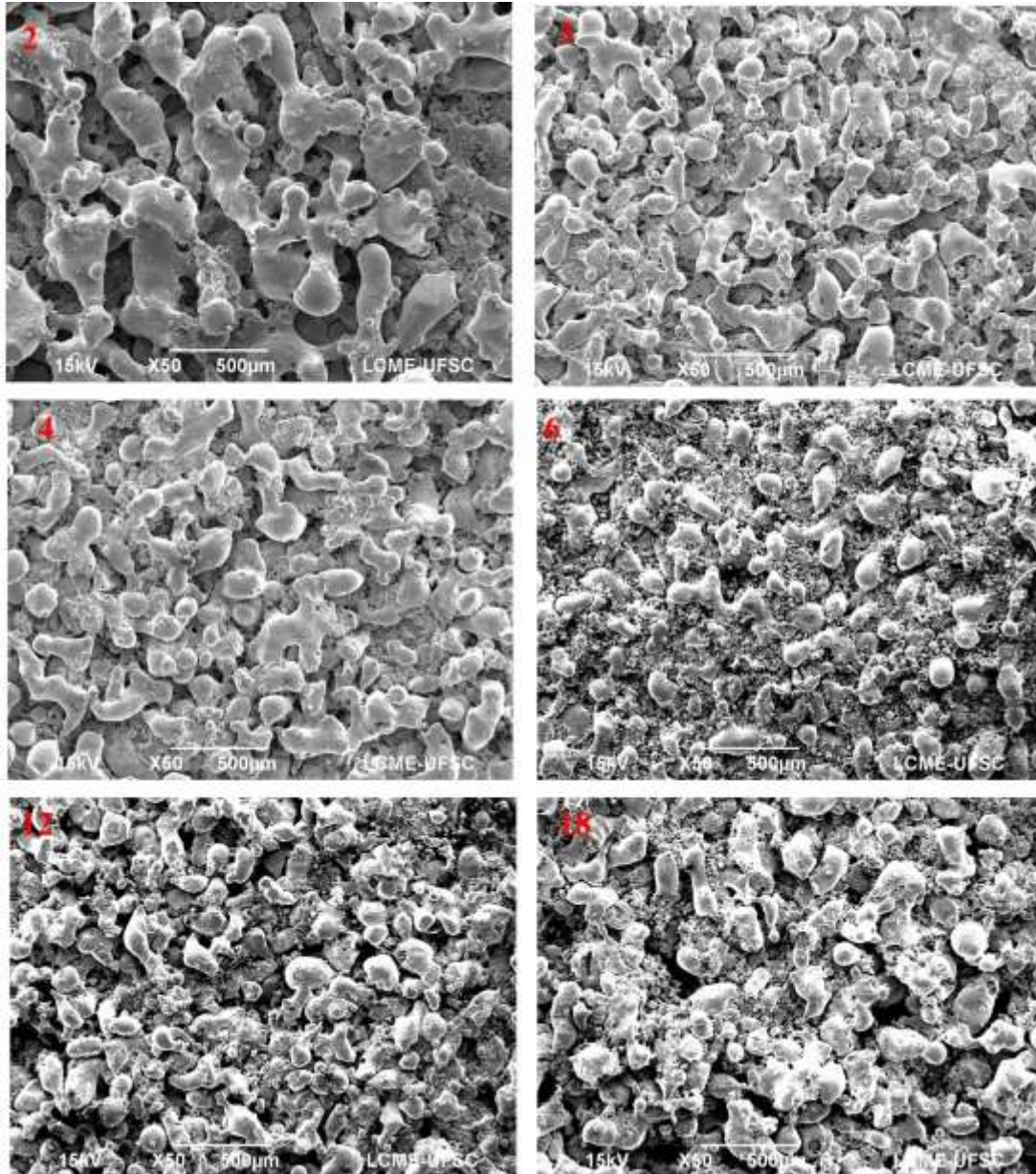


Figure 8: SEM analysis of six copper specimens, 50X.

The samples showed a very porous structure with difficulties on completing melt. This can be explained by analyzing copper powder SEM images – the powder was water atomized, therefore does not present a round shape. This lack of roundness of the particles also explains the behavior of powder flowability on the layer bed during manufacture. Particles with heterogeneous shape require different energies in different regions of each sample, in addition to the need for higher energy to complete melting due to a larger surface area. In sample 2 it is possible to see a weld direction behavior in a short length of the structure. The other samples, however, presented a quite heterogeneous and porous structure. Every sample taken to SEM analysis presented necks, but it is more visible in specimens 2, 3, 4 and 12. Samples 6 and 18 presented more loose particles, which can be easily removed if a mechanical force is applied.

SEM images agree to the consolidation analysis results – the samples are very porous, and a higher energy output is needed in order to obtain a better consolidation. It is also important to highlight copper reflectivity behavior even when fiber laser light is applied – this metal reflects 41% of the energy applied when a laser beam of wavelength equal to 1.06 μm is applied; if a wavelength of 10.6 μm (CO_2 laser) is used, copper reflects 74% (Santos et al. 2006).

Samples 2, 3, 12 and 18 were also taken to microstructure evaluation by using optic microscopy. Figure 9 and Figure 10 show the images obtained, respectively, before and after etching.

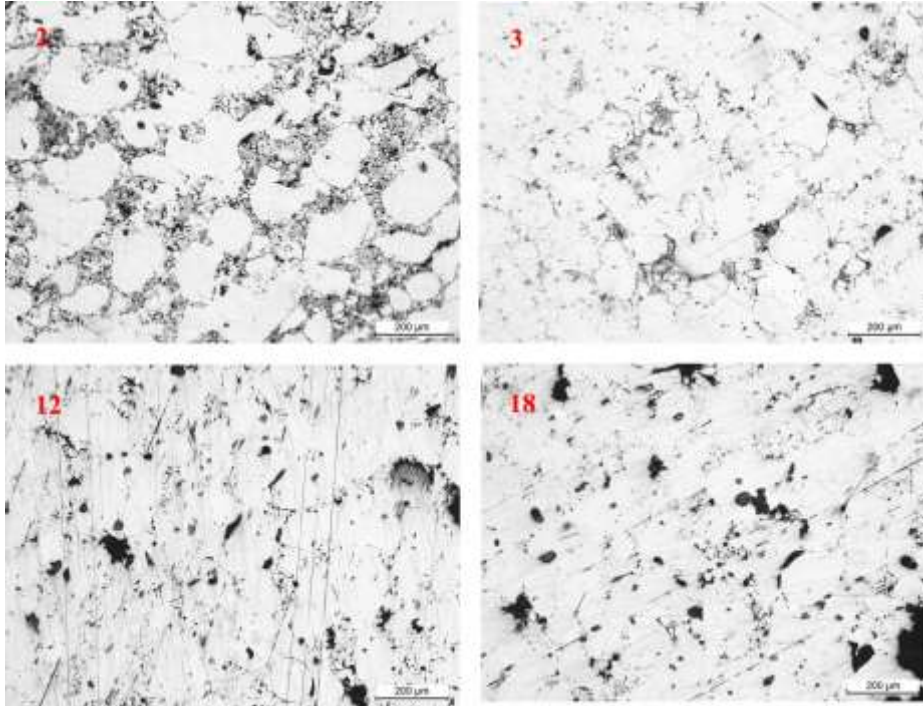


Figure 9: Microstructure of copper samples before etching.

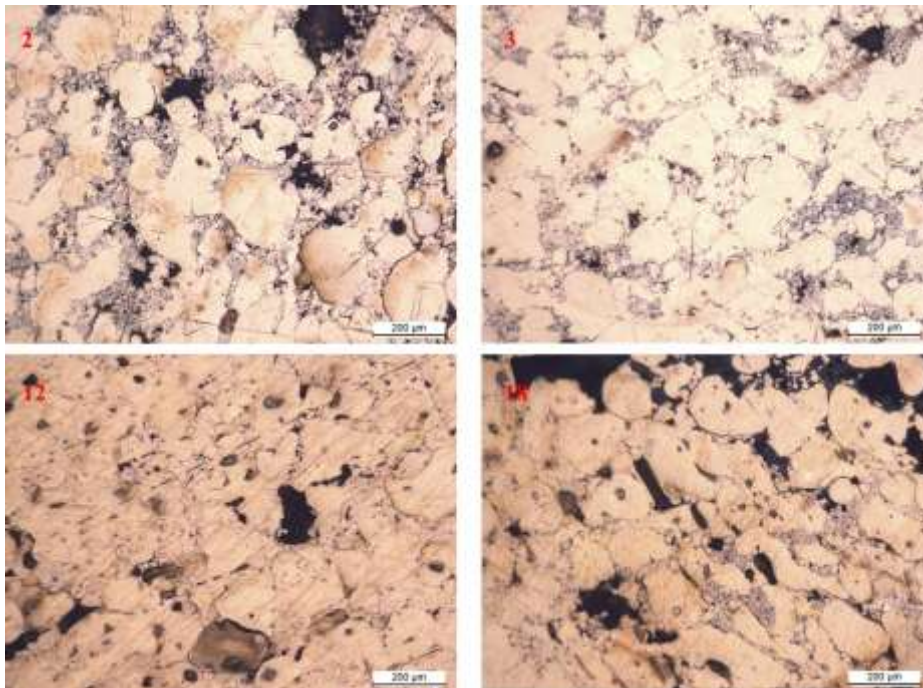


Figure 10: Microstructure of copper samples after etching.

The specimens appear to be more consolidated when analyzed by optic microscopy. This is due to sample preparation, which dragged loose particles to the top of previous layers. Even with particle dragging, some pores are still visible in the structure, which also compromise the mechanical properties. The grains have heterogeneous size with a maximum length of 300µm. A few pores are visible between layers, which support the lack of energy applied in order to melt the previous layers and build one single structure. Pores are also visible along the same layer, probably as a result of particle heterogeneity and low energy application.

The same specimens taken to SEM analysis were also taken to hardness evaluation. The results are shown in Figure 11.

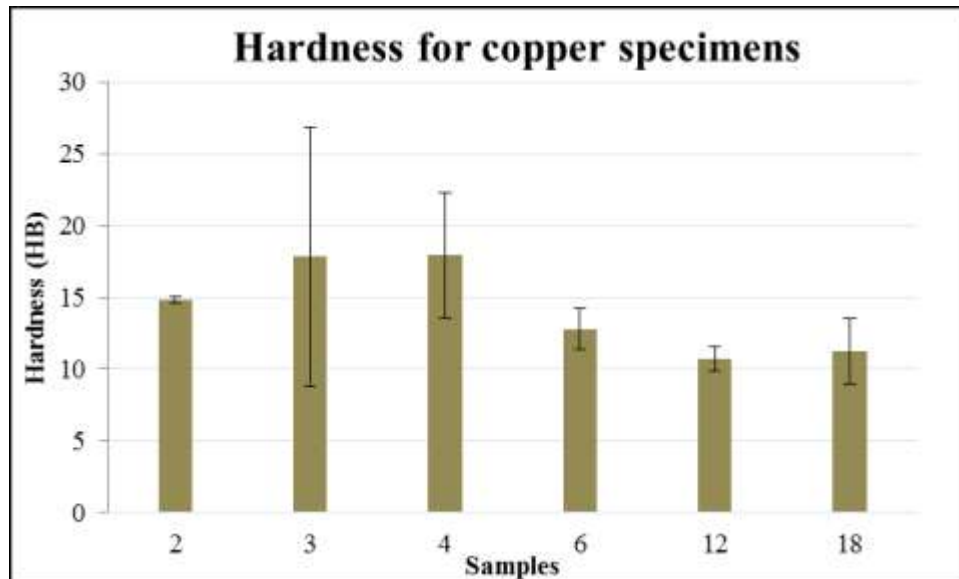


Figure 11: Hardness achieved for copper specimens.

The specimens' hardness are quite low if compared to the usual soft copper hardness of 43HB. The Brinell method was used in order to reduce the influence of structure heterogeneity, even though some specimens presented a quite high standard deviation, such as specimens 3 and 4. These specimens also showed the greatest hardness of all the specimens under evaluation. They achieved approximately 42% of the original hardness, while specimen 12 has shown the lowest hardness of 10.77 HB, correspondent to 25% of copper general hardness.

4. CONCLUSION

As mentioned in literature, some difficulties were found to process copper by SLM due to its high reflectivity and thermal conductivity. The parameters chosen have influenced the final mechanical performance and consolidation. The remelting technique proved to have an important role in specimen consolidation, increasing densification when applied once, but decreasing it when applied twice. The 94 W fiber laser used to apply the necessary energy to melt the copper powder proved to be insufficient. The final performance of all the specimens were quite low – all the specimens presented more than 50% of porosity, concluding that more energy and power output is needed to process copper by SLM. Finally, the mechanical performance has found to be low. This result could be predicted since the samples did not show a good consolidation. Even though similar results were achieved, it was still possible to find a correlation between the parameters applied and the results obtained. The hardness has shown a weak correlation of 0.4072 with the specimens' final consolidation.

5. ACKNOWLEDGEMENTS

The authors thank the Federal University of Santa Catarina, the NIMMA laboratory and the department of Mechanical Engineering for the support given to carry out this study.

6. REFERENCES

- ASTM International, 2013. "Standard Test Methods for Flow Rate of Metal Powders Using the Hall Flowmeter Funnel." <http://www.astm.org/Standards/B213.htm>.
———. 2015. "ASTM F2792-12a: Standard Terminology for Additive Manufacturing Technologies,": 3.

- Berzins, M., Childs, T.H.C., and Ryder, G.R., 1996. "The Selective Laser Sintering of Poly- Carbonate." *Annals of the CIRP* 45(1): 187–90.
- Bourell, D. L., Watt, T. J., Leigh, D. K., and Fulcher, B., 2014. "Performance Limitations in Polymer Laser Sintering." *Physics Procedia* 56: 147–56. <http://linkinghub.elsevier.com/retrieve/pii/S1875389214003022>.
- Childs, T. H. C., Berzins, M., Ryder, G.R., and Tontowi, A.E., 1999. "Selective Laser Sintering of an Amorphous Polymer: Simulations and Experiments." Part B: *Journal of Engineering Manufacture* 213: 333–49.
- Childs, T. H. C., and Tontowi, A.E., 2001. "No Title Selective Laser Sintering of a Crystalline and a Glass-Filled Crystalline Polymer: Experiments and Simulations." Part B: *Journal of Engineering Manufacture* 215: 1481–95.
- Drummer, D., Wudy, K., Kühnlein, F., and Drexler, M., 2012. "Polymer Blends for Selective Laser Sintering: Material and Process Requirements." *Physics Procedia* 39: 509–17. <http://www.sciencedirect.com/science/article/pii/S1875389212025941>.
- Franco, A., Lanzetta, M., and Romoli, L., 2010. "Experimental Analysis of Selective Laser Sintering of Polyamide Powders: An Energy Perspective." *Journal of Cleaner Production* 18(16–17): 1722–30. <http://dx.doi.org/10.1016/j.jclepro.2010.07.018>.
- Gu, D., Meiners, W., Wissenbach, K., and Poprawe, R., 2012. "Laser Additive Manufacturing of Metallic Components: Materials, Processes and Mechanisms." *International Materials Reviews* 57(3): 133–64.
- Gu, D. D. , Shen, Y., Fang, S., and Xiao, J., 2007. "Metallurgical Mechanisms in Direct Laser Sintering of Cu – CuSn – CuP Mixed Powder." *Journal of Alloys and Compounds* 438: 184–89.
- Gustmann, T. et al., 2016. "Influence of Processing Parameters on the Fabrication of a Cu-Al-Ni-Mn Shape-Memory Alloy by Selective Laser Melting." *Additive Manufacturing* 11: 23–31. <http://dx.doi.org/10.1016/j.addma.2016.04.003>.
- Hon, K. K. B., and Gill, T. J., 2003. "Selective Laser Sintering of SiC/polyamide Composites." *Annals of the CIRP* 52(1): 173–76.
- Kruth, J. P., Levy, G., Klocke, F., and Childs, T. H. C., 2007. "Consolidation Phenomena in Laser and Powder-Bed Based Layered Manufacturing." *CIRP Annals - Manufacturing Technology* 56(2): 730–59.
- Liu, Z. H. et al., 2014. "Interfacial Characterization of SLM Parts in Multi-Material Processing: Intermetallic Phase Formation between AlSi10Mg and C18400 Copper Alloy." *Materials Characterization* 107: 116–25. <http://dx.doi.org/10.1016/j.matchar.2014.05.001>.
- Lodes, M. A., Guschlbauer, R., and Korner C., 2015. "Process Development for the Manufacturing of 99.94% Pure Copper via Selective Electron Beam Melting." *Materials Letters* 143: 298–301. <http://dx.doi.org/10.1016/j.matlet.2014.12.105>.
- Lykov, P. A., Safonov, E. V., Akhmedjanov, A. M., 2016. "Selective Laser Melting of Copper." *Trans Tech Publications* 843: 284–88.
- Popovich, A. et al., 2016. "Microstructure and Mechanical Properties of Additive Manufactured Copper Alloy." *Materials Letters* 179: 38–41. <http://linkinghub.elsevier.com/retrieve/pii/S0167577X16307819>.
- Santos, E. C., Shiomi, M., Osakada, K., and Laoui, T., 2006. "Rapid Manufacturing of Metal Components by Laser Forming." *International Journal of Machine Tools and Manufacture* 46(12–13): 1459–68.
- Schmidt, M., Pohle, D., and Rechtenwald, T., 2007. "Selective Laser Sintering of PEEK." *CIRP Annals - Manufacturing Technology* 56(1): 205–8.
- da Silva, M. R. et al., 2016. "Laser Surface Remelting of a Cu-Al-Ni-Mn Shape Memory Alloy." *Materials Science and Engineering A* 661: 61–67. <http://dx.doi.org/10.1016/j.msea.2016.03.021>.
- Tang, Y. et al., 2003. "Direct Laser Sintering of a Copper-Based Alloy for Creating Three-Dimensional Metal Parts." *Materials Processing Technology* 140: 368–72.
- Thompson, S. M., Bian, L., Shamsaei, N., and Yadollahi, A., 2015. "An Overview of Direct Laser Deposition for Additive Manufacturing Part I: Transport Phenomena, Modeling and Diagnostics." *Additive Manufacturing* 31(7): 1–110. <http://linkinghub.elsevier.com/retrieve/pii/S2214860415000317>.
- Vinod, A. R., and Srinivasa, C. K., 2014. "Studies on Laser-Sintering of Copper by Direct Metal Laser Sintering Process." *Proceedings of the 5th International & 26th All India Manufacturing Technology, Design and Research Conference (AIMTDR 2014) (Aimtdr):* 377-1–4. http://www.iitg.ernet.in/aimtdr2014/PROCEEDINGS/papers/377.pdf%5Cnhttp://www.iitg.ernet.in/aimtdr2014/PROCEEDINGS/html/papers_adv_manfg_laser.html.
- Zhu, H. H., Lu, L., and Fuh, J. Y. H., 2003. "Development and Characterisation of Direct Laser Sintering Cu-Based Metal Powder." *Materials Processing Technology* 140: 314–17.

7. RESPONSIBILITY NOTICE

The authors are the only responsables for the printed material included in this paper.